



## Geo-Hazard Assessment and Mapping In Barangay Kiorao, Kibawe, Bukidnon

*Ma. Catherine Q. Arca, Cheryl F. Daleon, Eric L. Cenabre, Einstine M. Opiso,  
Paulino R. Reomero, Richie Catherine Supremo-Lood, Richard Namuag,  
Methuselah Gen R. Berame, and Jan Mavylle S. Umali*

Department of Civil Engineering, College of Engineering, Central Mindanao University  
Musuan, Bukidnon, Philippines, 8710

### ABSTRACT

Geohazards pose a significant threat to human life and property in the Philippines, and Barangay Kiorao, Bukidnon is no exception. Predominantly expansive soils in the barangay are susceptible to swelling and shrinking with changes in moisture content, and three sampling areas were identified to be collapsible. These soil conditions, combined with the barangay's location in a seismically active region, render it vulnerable to a variety of geohazards, including landslides and earthquakes. This study aimed to generate a geohazard map of the barangay to inform land use planning and disaster risk reduction efforts. Slope stability analysis revealed that the slopes in Barangay Kiorao are stable under semi-saturated and fully saturated conditions, even with friction angles as low as  $0^\circ$ . This suggests that the slopes have a "high" to a "very high" stability even under extreme conditions. Despite being safe from ground rupture, liquefaction, and tsunami, Barangay Kiorao is susceptible to strong ground shaking during earthquakes. The seismic hazard assessment identified areas in the Barangay that are at risk of experiencing strong ground motions during earthquakes. The resulting geohazard map scaled at 1:200,000 integrated these findings, marking areas susceptible to landslide and earthquakes.

*Keywords:* factor of safety, geohazard mapping, shallow landslides, slope stability, soil thickness

### INTRODUCTION

Geohazards, encompassing a wide range of natural processes, can have a significant impact on human activities around the world. Advances in geohazard mapping have improved the ability to assess and mitigate these risks. However, the rapid development of infrastructures in vulnerable areas often outpaces the creation of effective disaster preparedness strategies. A critical gap remains in accounting for the dynamic environmental and geological changes that can render existing hazard maps obsolete. The Philippines, situated on the typhoon belt and along the Pacific Ring of Fire, is a testament to the complexity of managing geohazards (Aurelio, 2004). The country's topography and climatic conditions predispose it to a variety of hazard, with landslides frequently occurring in areas with steep slopes and high rainfall. These events are exacerbated by geological materials that are weathered and structurally weak, leading to numerous forms of slope failure (Padrones, et al., 2017). The commonly observed slope failures in the country include block slides, debris slides, and earth creep (Opiso et al., 2016). Moreover, seismic activities present additional risks. Seismic hazard is used to characterize earthquake-induced natural processes that can be harmful, such as surface rupture, ground motion, ground-motion amplification, liquefaction, or triggered landslides (Wang, 2011). The July 2023 mudflow, which triggered a flash flood, and the series of earthquakes from June to July 2023 underscore Kibawe, Bukidnon's vulnerability to a variety of geohazards. These events serve as stark reminders of the urgent need for comprehensive and effective disaster risk reduction strategies to safeguard the lives and property of Kibawe residents.

conducting a slope stability assessment, identifying problematic soils, identifying locations vulnerable to earthquakes, and ultimately, developing a detailed geohazard map for Barangay Kiorao in Kibawe, Bukidnon. This supports the ongoing efforts to improve mobility and connectivity in the area. By employing a deterministic quantitative approach through Infinite Slope Model, this study evaluates slope stability and identifies regions at heightened risk, incorporating soil properties, slope gradients, and saturation levels into the analysis. This model is a well-established method for calculating the Factor of Safety (FS) for shallow landslide assessment. The FS is a measure of how stable a slope is. A lower FS indicates a higher risk of landslides. Additionally, the study also considered seismic hazards. Accessible data from HazardHunterPH, a tool developed by the Philippine Institute of Volcanology and Seismology, was incorporated into the geohazard map to identify areas prone to ground shaking, liquefaction, and tsunami. Leveraging Geographic Information System (GIS) techniques in mapping provides an excellent tool for assessing potential risks. GIS is a computer-based tool that allows the creation of detailed maps by combining different types of data. This helps in visualizing and understanding the potential impact of geohazards on communities.

The resulting geohazard map is a step towards bridging the information gap for communities, policy makers, and developers. It serves as a vital tool for disaster risk management, enabling the formulation of

#### Corresponding author:

Ma. Catherine Q. Arca

Email Address: cathiearc1580@gmail.com

Received: Apr. 14, 2023 ; Accepted: Oct. 10, 2023

This study addresses these challenges by

effective mitigation strategies and emergency response plans. Identifying areas at risk equips communities, local government units, and developers with the information they need to make informed decisions, steering growth towards safer zones. Ultimately, the purpose of this study is to foster development of resilient communities, safeguarding lives and property against the inevitable challenges posed by natural hazards in the Philippines.

## METHODOLOGY

### Study Area

The research area is in Barangay Kiorao, found in the Municipality of Kibawe, in the province of Bukidnon, in Region X, Northern Mindanao, the Philippines. Kibawe has a more significant percentage of rolling than plain areas. A rough estimate is 80% rolling hills and 20% plainlands. The important landmarks of the municipality are several mountain peaks clustered over most of the barangays. On the island of Mindanao, Barangay Kiorao is located roughly 7° 31' North and 124° 55' East. The elevation at these coordinates is estimated to be 275.1 meters, or 902.5 feet, above mean sea level. As determined by the 2020 Census, Barangay Kiorao had a population of 653, accounting for 1.56% of Kibawe's total population.

The geology of Barangay Kiorao is complex, with a mix of volcanic and sedimentary rocks. The volcanic rocks

in the barangay are predominantly andesite and basalt. The sedimentary rocks in the barangay include sandstone, shale, and limestone. The soil types in Barangay Kiorao are also varied. The most common soil type is clayey soil, which is often found on steep slopes. Sandy soils are also common in the barangay, especially in areas that are prone to flooding. Loamy soils are found in areas that are well-drained and have a mix of sand, silt, and clay. The rainforest in the barangay is dominated by trees such as dipterocarps, mahogany, and narra. The grassland in the barangay is dominated by grasses such as cogon and elephant grasses.

An initial inspection of the study area was conducted to evaluate its accessibility and to account for all the industrial and agricultural establishments, road networks, and communities at high risk of a geohazard. The findings of the initial inspection suggests that Barangay Kiorao is vulnerable to a variety of geohazards, including landslides and earthquakes. The risk of geohazards is exacerbated by the barangay's complex geology, steep slopes, and varied soil types.

### Generation of Slope Map

GIS exploration was conducted to obtain data on slope gradient. A 5x5 meter resolution Digital Elevation Model (DEM) was procured from the National Mapping and Resource Information Authority (NAMRIA) through

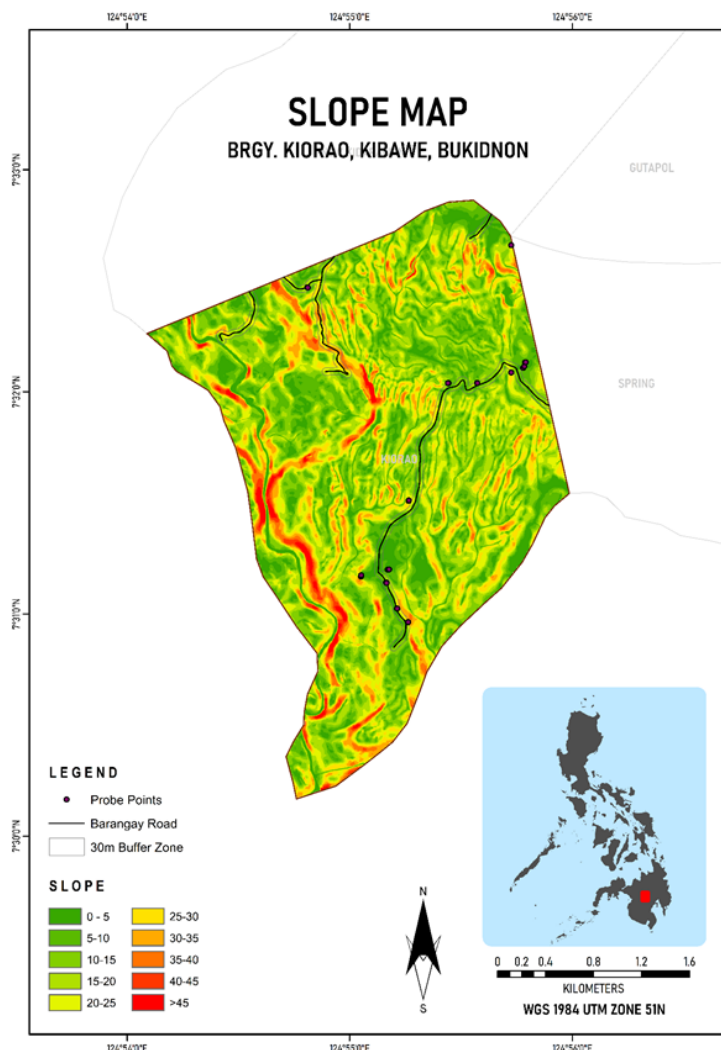


Figure 1. Slope Map of Barangay Kiorao.

the Central Mindanao University (CMU) GeoMin Center. The DEM was used to generate a slope map of the study area, which showed that slope angle was a major factor influencing slope stability. The slope variability in the study area was derived using ArcGIS software, as shown in figure 1.

Sampling points were deliberately chosen near roads to ensure the safety of the field team and expedite data collection. Some parts of the barangay were inaccessible by car, and others were too dangerous to reach during the rainy season. By focusing sampling near roads, the team was able to optimize resources and collect quality data without overspending. Despite their proximity to roads, the sampling points represented a wide range of slope angles. This was important because roads often lead to or area adjacent to population centers, which are at heightened risk of slope instability due to increased human activity and potential infrastructural developments.

### *Soil Sampling*

Soil samples were collected from across the study area to determine the necessary geotechnical properties. The selection of sampling points was based on slope gradients, as indicated by slope map data. Different slope gradients can significantly influence soil properties, so it was important to capture samples from various slope categories. To systematically identify sampling points, the study area was stratified into distinct slope gradient ranges. Within each gradient stratum, specific locations were chosen to capture the variability of soil conditions influenced by that particular slope range. The soil was then characterized in terms of its physical, index, and mechanical properties. The soil sampling procedure adhered to ASTM D1452-09 standards. Before sampling, the chosen area was cleared of any debris and vegetation. Disturbed soil samples were collected and immediately sealed in airtight containers to preserve their moisture content. These samples were tested in the laboratory to determine index properties such as Atterberg limits, moisture content, dry density, and particle size distribution. Core samplers were used at the predetermined sampling points to obtain undisturbed soil samples, which were similarly sealed to maintain their moisture levels. These undisturbed samples were essential for determining the soil's shear strength parameters. The soil sampling method ensured that the samples collected provided a representative overview of the soil properties across different slope gradients in the study area.

### *Determination of the Geotechnical Properties of the Soil*

To comprehensively understand the geotechnical properties of the soil samples collected from the study area, a systematic approach was adopted, targeting the determination of moisture content, particle size distribution, soil classification based on index properties, Atterberg limits, unit weight, and key parameters such as soil density, cohesion, and internal friction angle. The moisture content of disturbed soil samples was determined in accordance with ASTM D2216 using standard oven-drying procedures. This involved heating the samples to 110°C for 24 hours in a thermoelectric oven. Sieve analysis was performed on the oven-dried

soil samples to determine their particle size distribution, as per ASTM D422. The resulting particle size distribution was classified following the guidelines of ASTM D2487-11, the Unified Soil Classification System (USCS), and the American Association of State Highway and Transportation Officials (AASHTO) standard classification. The index properties of the disturbed soil samples were evaluated to facilitate soil classification. The Atterberg limits, indicative of the soil's plasticity, were determined using the fall cone method, following ASTM D4318. The total unit weight of the undisturbed soil samples was determined in accordance with ASTM D2937. This involved extruding the samples from the core samples using a soil extruder and measuring their weight and dimensions using a vernier caliper. To determine the shear strength parameters of the undisturbed soil samples, a Direct Shear Test under Consolidated Drained Conditions was performed, as per ASTM D3080. This test provided vital data on soil density, cohesion, and internal friction angle. The data amassed from these laboratory tests offered a holistic view of the geotechnical parameters of the soil samples, facilitating a robust analysis and correlation of their properties.

### *Slope Stability Assessment*

Slope stability assessment is the process of determining and evaluating how much stress a specific slope can withstand before failing. It is a fundamental step in evaluating landslide hazards and designing safe structures. The slope stability assessment in this study was conducted using the Infinite Slope Model (ISM) through an Excel spreadsheet. The ISM is a simple but effective model for assessing slope stability. However, it is important to note that it is a deterministic model that assumes a uniform slope and infinite length. In reality, slopes are often heterogeneous and finite. This can lead to inaccuracies in the slope stability assessments produced using the ISM. Despite its limitations, the ISM was chosen for this study because it is a well-established and widely used model for slope stability analysis. Additionally, the ISM is relatively easy to use and does not require a large amount of data. The following critical input parameters were used to assess slope stability using the ISM:

Unit Weight of soil ( $\gamma$ ): This parameter represents the density of the soil, which is a fundamental factor in calculating the gravitational forces acting on the slope.  
Saturation Index ( $m$ ): also known as groundwater depth to soil thickness ratio. This ratio indicates the level of soil saturation with water, where 'zw' is the height of the water table above the failure surface, and 'z' is the depth of the failure surface below the terrain surface (Mondal & Maiti, 2012).

Cohesion ( $c$ ): This soil strength parameter represents the resistance to shear due to interparticle bonding.

Angle of Internal friction ( $\phi$ ): This soil strength parameter represents the resistance to shear due to interlocking of soil particles.

Terrain Surface Inclination ( $\beta$ ): The angle of the slope with respect to the horizontal plane, which directly affects the potential for slope movement.

To establish the relationship between soil parameters and slope angle, empirical relationships from Daleon & Lorenzo (2018) were used, as direct measurements were not possible at all sampling points. This approach was necessitated by financial constraints that limited the number of direct shear tests to four sampling points. For these four points, the measured values of cohesion and angle of internal friction angle were directly used in the Factor of Safety (FS) calculations. For the remaining points, the correlations were used to estimate these parameters, allowing for a comprehensive analysis across all 13 sampling points.

The FS is defined as the ratio of resisting forces to driving forces along the potential failure surface, with FS = 1.0 indicating imminent failure (Chae et al., 2015). An FS less than 1.0 suggests an unstable slope, necessitating intervention. The factor of safety is calculated according to the following formula of Brunsden & Prior (1979):

$$FS = \frac{c' + (\gamma - m\gamma_w)z\cos^2\beta\tan\Phi'}{\gamma z\sin\beta\cos\beta}$$

Where:

- c' – is the effective cohesion
- γ – unit weight of soil
- γ<sub>w</sub> – unit weight of water
- m – z<sub>w</sub>/z
- z – depth of the failure surface below the surface (m)
- z<sub>w</sub> – height of water table above failure surface (m)
- β – slope surface inclination
- Φ' – effective angle of shearing resistance

The FS was calculated at incremental 2-degree intervals of slope inclination. This incremental approach commenced at a minimal slope angle of 2 degrees and progressed methodically to the actual slope angle observed at each sampling point. By adopting this interval-based calculation, the study was able to capture the FS for a range of potential slope inclinations, providing a nuanced understanding of how slope stability varies with changes in slope angle.

Groundwater's role in slope stability was accounted for by considering different saturation conditions: semi-saturated (m<sub>1</sub> = 0.5, m<sub>2</sub> = 0.25) and fully saturated (m = 1). For the fully saturated condition, the friction angle was reduced to account for the increase in water content. This assumption was based on the inverse relationship between friction angle and moisture content, which shows that the friction angle tends to decrease with increasing moisture content (Arca & Lorenzo, 2018), see figure 2. These conditions simulate the fluctuating groundwater table, particularly during the monsoon season, when rainwater infiltration can raise water levels and increase pore water pressure, thereby reducing slope stability.

ArcGIS was used to map the calculated FS values, providing a visual representation of slope stability across the study area. As shown in table 1, the FS values were categorized into different stability classes as per the Factor of Safety Classification by Arca & Lorenzo (2018), facilitating the interpretation of stability and spatial distribution risk.

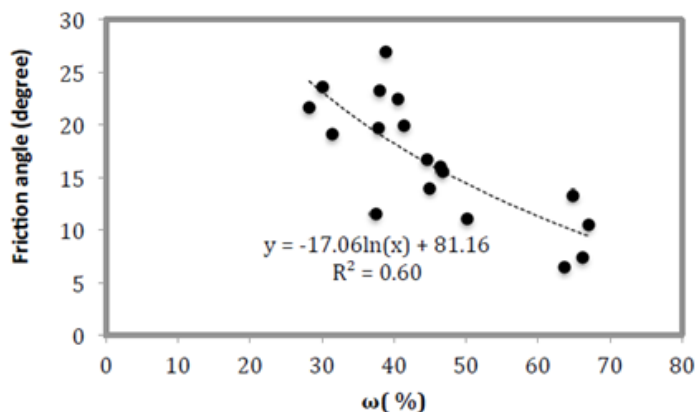


Figure 2. Logarithmic w-Φ Curve (Arca & Lorenzo, 2018).

Table 1. Factor of Safety Classification (Arca & Lorenzo, 2018).

Color Code	Factor of Safety	Stability Class
	0 - 0.50	Unstable
	0.50 - 1.00	Very Low
	1.00 - 1.25	Low
	1.25 - 1.50	Moderate
	1.50 - 2.00	High
	> 2.00	Very High

Table 2. Soil Expansivity Prediction by Liquid Limit.

Degree of expansion	$w_L$ : %	
	Chen <sup>6</sup>	IS 1498 <sup>4</sup>
Low	< 30	20–35
Medium	30–40	35–50
High	40–60	50–70
Very high	> 60	70–90

Table 3. Soil Expansivity Prediction by Plasticity Index.

Degree of expansion	$I_p$ : %		
	Holtz and Gibbs <sup>10</sup>	Chen <sup>6</sup>	IS 1498 <sup>4</sup>
Low	< 20	0–15	< 12
Medium	12–34	10–35	12–23
High	23–45	20–55	23–32
Very high	> 32	> 35	> 32

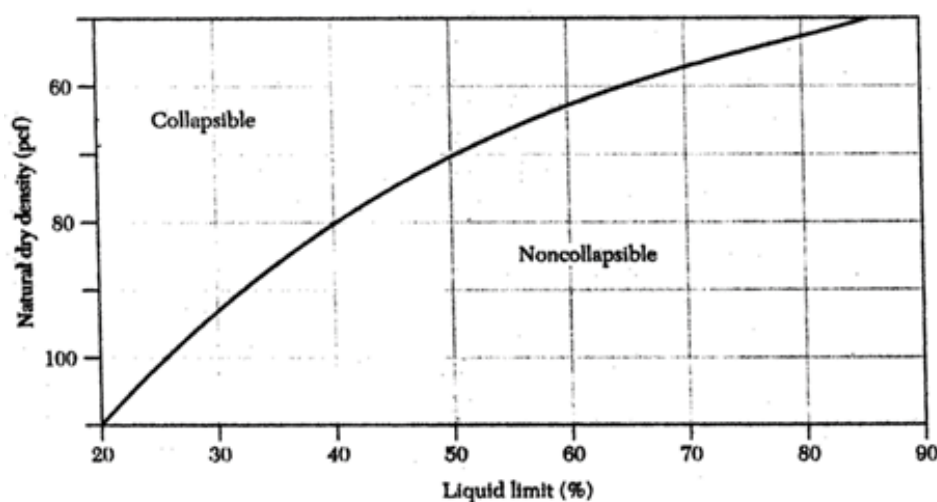


Figure 3. Criterion for Collapsibility Potential (Holtz & Gibbs, 1967).

#### Determination of Problematic Soil

According to Baynes (2008), expansive soils, soft clays, collapsible soils, and dispersive soils are among the most problematic soils. This study focused on identifying and characterizing expansive and collapsible soils. Expansive soils experience significant volume changes in response to moisture fluctuations. To predict soil expansivity, two key geotechnical properties were measured: the liquid limit and the plasticity index. The liquid limit is the water content at which soil transitions from a plastic to a liquid state. The liquid limit and plasticity index were cross-referenced with the soil expansivity prediction tables developed by Chen (1983) and Holtz and Gibbs (1967), respectively (see Tables 2 and 3). These tables classify expansivity potential based on the measured liquid limit and plasticity index values, enabling a quantitative assessment of the soil's expansive nature. By integrating these two predictive tables, the study leverages robust, empirically derived data to classify

soil expansivity and facilitate a more informed evaluation of the risks associated with soil volume changes in the study area.

On the other hand, the primary concern with collapsible soils is the significant loss of shear strength and volume reduction that occurs when they are exposed to more water or moisture. The collapsibility of the soil in the study area was assessed using the criterion for collapsible potential provided by Holtz and Gibbs (1967), as presented in 3. This criterion entails measuring the soil's natural moisture content, dry unit weight, and degree of saturation. Collapsible soils typically have a low natural moisture content, low dry unit weight, and are frequently only partially saturated. When these soils become wet, the interparticle bonds that provide structure and strength can weaken or dissolve, resulting in a sudden and significant decrease in volume and bearing capacity. The degree of collapse is then used to classify the soil's collapsibility

potential, which can range from non-collapsible to highly collapsible.

### Geohazard Mapping

The geohazard mapping was systematically conducted using ArcGIS software to integrate various datasets and to visualize the spatial variability of potential risks. Initially, a field reconnaissance survey was undertaken to gather first-hand observations of the current geohazard conditions and to document the historical geohazard events within the study area. Various data sets, including those pertaining to soil properties, slope stability, and historical geohazard events were compiled. This data served as the foundation for the subsequent analysis.

The Infinite Slope Model (ISM) was used to generate slope stability maps for the study area. Two (2) sets of FS maps were generated to represent semi-saturated conditions with saturation indices of  $m_1 = 0.25$  and  $m_2 = 0.5$ . Additionally, five (5) FS maps were produced to model the slope stability under fully saturated conditions with varying friction angles ( $\Phi_1 = 2.4$ ,  $\Phi_2 = 4.4$ ,  $\Phi_3 = 6.4$ ,  $\Phi_4 = 8.7$ , and  $\Phi_5 = 0$ ), the latter to simulate the worst-case scenario. HazardHunterPH, a collaborative product of GeoRisk Philippines, was employed to generate the preliminary hazard assessment reports for the study area. This tool provided insights into the potential impact of geological hazards on the community.

Shapefiles indicating liquefaction susceptibility, active faults, and potentially active faults were obtained from PHIVOLCS. These shapefiles contain critical geospatial information necessary for the hazard mapping. The acquired shapefiles were then overlaid on the FS map that depicted the fully saturated condition with a friction angle of zero. This overlay process was meticulously performed to ensure that the spatial correlation between the FS data and the geohazard indicators was accurately represented. The final step involved the synthesis of the overlaid data to produce a comprehensive Geohazard Map. This map illustrates the areas of potential risk by combining the slope stability data with the geohazard indicators from the shapefiles.

## RESULTS AND DISCUSSION

### Geotechnical Data

The physical properties of the soil within the study area, as detailed in Table 4, provide valuable insights into the collapsibility potential of the soils encountered. The average moisture content of 46.44% is indicative of a moderate to high level of soil moisture, which is a critical determinant of soil behavior. Moisture content significantly influences soil compressibility, permeability, and strength. In the context of collapsibility, the high moisture content observed in the study area could be a precursor to increased soil compressibility and a reduction in shear strength (Ian & Chris DF, 2012). This is because water acts as a lubricant between soil particles, diminishing the interparticle friction that provide shear resistance (Bláhová et al., 2013).

The average total unit weight of the soil, recorded at 15.55 kN/m<sup>3</sup>, and the dry unit weight, at 10.63 kN/m<sup>3</sup>, are also significant in assessing the collapsibility potential. The unit weight of soil is a fundamental parameter that affects the bearing capacity and settlement characteristics of the soil. In the case of collapsible soils, the dry unit weight can be particularly telling. A low dry unit weight often corresponds to a loosely packed soil structure, which is susceptible to collapse when the soil becomes wet and capillary stresses are diminished, as described in the Soil Mechanics Designs Manual 7.01 (1986).

It is also important to note that the sample points fall within different slope categories, ranging from gentler to mid-portion slopes (6° to 41°) and steep slopes greater than 45°. This information is crucial for assessing the potential impact of slope angle on soil stability and the risk of landslides or collapse. The identification of BH8, BH11, and BH12 as collapsible soils, based on the Holtz and Gibbs criteria, underscores the importance of these physical properties. When these soils are exposed to moisture, such as during construction activities or changes in groundwater levels, the potential for rapid settlement or collapse becomes a critical consideration for land development and infrastructure design.

Table 4. Physical Properties and Collapsibility of the Soil Samples.

Sampling Code	Slope (°)	Moisture Content (%)	Density (kg/m <sup>3</sup> )	Total Unit Weight (kN/m <sup>3</sup> )	Dry Unit Weight (kN/m <sup>3</sup> )	Liquid Limit (%)	Collapsibility
BH1	6	49.71	1,533.96	15.05	10.05	64.90	N
BH2	11	43.68	1,709.91	16.77	11.67	74.99	N
BH3	13	43.89	1,572.59	15.43	10.72	75.98	N
BH4	20	48.63	1,616.81	15.86	10.67	50.57	N
BH5	21	48.24	1,550.66	15.21	10.26	56.36	N
BH6	26	49.75	1,632.65	16.02	10.70	68.27	N
BH7	27	42.33	1,654.61	16.23	11.40	47.38	N
BH8	31	56.63	1,660.00	16.28	10.40	57.93	C-C
BH9	38	48.75	1,583.94	15.54	10.45	80.09	N
BH10	41	53.91	1,462.17	14.34	9.32	89.12	N
BH11	48	40.00	1,591.62	15.61	11.15	44.57	C-C
BH12	51	36.74	1,511.82	14.83	10.85	47.15	C-C
BH13	53	41.52	1,522.44	14.94	10.55	52.53	N
<b>Average</b>		<b>46.44</b>	<b>1,584.86</b>	<b>15.55</b>	<b>10.63</b>	<b>62.30</b>	

The measurement of Atterberg limits is an essential part of soil analysis, as it provides valuable insights into the soil's behavior and potential for problems, such as expansion, under different moisture and clay content conditions (Selby, 1993; Mugagga, et al., 2011; Bidyashwari, et al., 2017). Table 5 presents the liquid limit, plasticity index, and liquidity index of the soils within the study area. The liquid limit, a critical parameter in soil mechanics, varies from 44.57% to 89.09%. This limit represents the moisture content at which soil transitions from plastic to liquid (O'Kelly, 2021). The average liquid limit for the study area is 62.30%. According to the classification provided by IS 1498, this average falls within the 50%-70% range, indicating a high degree of expansion. This high liquid limit suggests high compressibility and a significant shrinkage or swelling potential. These characteristics can significantly influence the soil's behavior under load and its response to changes in moisture content. The plasticity index, another critical parameter, ranges from 14.11% to 71.28%. This index measures the range of water content over which the soil exhibits plastic behavior. The observed range indicates that the soils in the study area show medium to very high plasticity. Soils with a plasticity index greater than 25 are classified as expansive, as described in ASTM D4318. These soils have a high potential for volume change with changes

in moisture content, which can lead to significant ground movement and potential damage to structures. Daleon (2022) corroborates these findings, identifying the majority of the soils in the study area as highly expansive with a high tendency to swell. This propensity for swelling can pose significant challenges for construction and requires careful consideration during the design and construction process. The liquidity index, which measures the natural water content of the soil relative to the liquid and plastic limits, varies from 0.26 to 0.96. This range indicates that the soil can deform like plastic under certain conditions. A high liquidity index suggests that the soil is closer to the liquid limit and is likely to exhibit significant deformation under load.

Table 6 presents the grain size distribution of the soil within the study area. A notable characteristic of the soil is its high clay and silt content, which ranges from 56.5% to 98.49%. This high percentage significantly exceeds the 32% threshold, indicating an extremely high expansive potential (Mugagga, et al., 2011; Baynes, 2008; Den Merwe, 1964). Expansive soils, also known as shrink-swell soils, undergo significant volume changes with changes in moisture content (Reddy et. al, 2020; and Kabeta & Lemma, 2023). Upon saturation, these soils

Table 5. Index Properties of the Soil Samples.

Sampling Code	Slope (°)	Liquid Limit (%)	Plastic Limit (%)	Plasticity Index (%)	Liquidity Index
BH1	6	64.9	36.29	28.61	0.47
BH2	11	74.99	19.67	55.32	0.43
BH3	13	75.98	28.02	47.96	0.33
BH4	20	50.57	14.56	36.01	0.95
BH5	21	56.36	36.75	19.61	0.59
BH6	26	68.27	16.59	51.68	0.64
BH7	27	47.38	31.10	16.28	0.69
BH8	31	57.93	24.78	33.15	0.96
BH9	38	80.09	20.87	59.22	0.47
BH10	41	89.12	17.84	71.28	0.51
BH11	48	44.57	26.73	17.84	0.74
BH12	51	47.15	33.04	14.11	0.26
BH13	53	52.53	25.29	27.24	0.60
<b>Average</b>		<b>62.30</b>	<b>25.50</b>	<b>36.79</b>	<b>0.59</b>

Table 6. Grain Size Distribution of the Soil Samples.

Sampling Code	Slope (°)	Coefficient of Uniformity, Cu	Coefficient of Concavity, Cc	Textural Composition (%)		
				Gravel	Sand	Clay and Silt
BH1	6	11.00	0.62	0.00	10.25	89.75
BH2	11	9.61	0.64	2.28	2.62	95.10
BH3	13	8.89	0.65	0.07	1.44	98.49
BH4	20	14.80	0.58	1.49	18.65	79.86
BH5	21	10.60	0.62	0.43	8.41	91.16
BH6	26	22.85	0.53	5.60	25.62	68.78
BH7	27	11.37	0.62	0.21	11.25	88.54
BH8	31	10.55	0.62	0.00	8.67	91.33
BH9	38	11.45	0.61	3.64	8.10	88.26
BH10	41	9.25	0.64	1.63	1.63	96.74
BH11	48	19.50	0.55	2.36	25.19	72.45
BH12	51	65.58	0.32	8.99	34.51	56.50
BH13	53	12.93	0.60	0.00	15.92	84.08

experience a sudden loss of strength. This loss of strength occurs as rainfall infiltration reduces soil suction and increases pore-water pressure, thereby reducing the soil's shear strength capacity. The soil's high clay and silt content significantly affects its behavior. While silt retains a large amount of water, clay tends to be very dense. Clay also has slow permeability, resulting in a substantial water-holding capacity. This capacity can lead to prolonged periods of high moisture content, influencing the soil's shrink-swell behavior and suitability for construction.

The soil also exhibits a varying Coefficient of Uniformity (Cu) value, ranging from 8.89 to 65.58. The Cu measures the range of particle sizes in a soil sample. A high Cu indicates well-graded soil with a wide range of particle sizes. At the same time, a low value suggests that the soil is poorly-graded with a narrow range of particle sizes. The Coefficient of Concavity (Cc) of the soil ranges from 0.32 to 0.65. This coefficient measures the curvature of the particle size distribution curve. It provides insights into the grading characteristics of the soil. Daleon (2022) classified the soil in the study area as gap-graded. Gap-graded soils have an excess or deficiency of specific particle sizes or may lack at least one particle size. This grading characteristic can influence the soil's compaction characteristics, permeability, and shear strength.

Table 7 presents the soil classification in the study area. The study identified three distinct types of soil in the area. The first type is MH, or elastic silt, a soil of high plasticity. Elastic silt is characterized by its ability to undergo significant deformation without cracking or breaking. This characteristic can influence the soil's response to loading and suitability for construction. High plasticity indicates that the soil can undergo significant changes in volume with changes in moisture, leading to ground movement and potential damage to structures.

The second type of soil identified in the study area is CH, or fat clay, with very high plasticity. Fat clay is known for its high water-holding capacity and ability to undergo significant volume changes with changes in moisture content. These characteristics can lead to considerable ground movement, posing challenges for construction and requiring careful engineering considerations.

The third type of soil is ML, or silt, a soil of medium plasticity. Silt is characterized by its fine particles and its ability to retain water. Medium plasticity indicates that the

soil can undergo moderate volume changes with changes in moisture content. While less reactive than high plasticity soils, medium plasticity soils can still pose challenges for construction, particularly in areas with significant changes in moisture content.

Table 8 presents the results of direct shear tests conducted on soil samples from four boreholes within the study area. The test determines the soil's shear strength parameters, specifically the cohesion and friction angle. These parameters are crucial for understanding the soil's behavior under shear stress and its suitability for construction. Financial constraints limited the direct shear tests to only four (4) boreholes. Despite this limitation, the tests provided valuable insights into the shear strength characteristics of the different soil types in the study area.

The CH soil type exhibited the highest cohesion value of 19.8 kN/m<sup>2</sup>. Cohesion measures the soil's ability to stick together and resist shear stress. A high cohesion value indicates a high resistance to shear stress, which can benefit supporting structures. However, the CH soil type had the lowest friction angle value of 10.8°. The friction angle measures the soil's internal resistance to sliding along a failure plane. A low friction angle suggests a lower resistance to sliding, which can influence the soil's stability under load. The ML soil type had an average cohesion value of 19.6 kN/m<sup>2</sup> and an average friction angle value of 11.85°. These values suggest a moderate resistance to shear stress and sliding, indicating a balance between cohesion and frictional resistance.

On the other hand, the MH soil type had the lowest cohesion value of 11.4 kN/m<sup>2</sup> but the highest friction angle value of 16.9°. Blahova et al. (2013) noted that cohesion usually does not increase with increasing stress, except for clayey soils. In these soils, an increase in stress can lead to an increase in molecular bonds, enhancing the soil's cohesion.

Daleon & Lorenzo (2018) previously established a correlation between several vital parameters: soil thickness with slope angle, cohesion with slope angle, and friction angle with slope angle. These correlations provide a robust framework for generating the necessary soil stability parameters for calculating the FS, a critical measure of slope stability. This study adapted these correlations to analyze the soils within the study area.

Table 7. Soil Classification.

Sampling Code	Slope (°)	Soil Classification		Description	Soil Type (Budhu, 2000)	Degree of Plasticity (Venkatramiah, 2006)
		USCS	AASHTO			
BH1	6	MH	A-7-5	Dark brown silts with few sands	Clay	High plasticity
BH2	11	CH	A-7-6	Dark brown clays with traces of sands & gravels	Clay	Very high plasticity
BH3	13	CH	A-7-6	Dark brown clays with traces of sands	Clay	Very high plasticity
BH4	20	CH	A-7-6	Dark brown clays with little sands & traces of gravels	Clay	Very high plasticity
BH5	21	MH	A-7-5	Dark yellowish brown silts with few sands	Clay	Medium plasticity
BH6	26	CH	A-7-6	Dark brown clays with little sands & traces of gravels	Clay	Very high plasticity
BH7	27	ML	A-7-5	Dark yellowish brown sandy silts	Clay	Medium plasticity
BH8	31	CH	A-7-6	Strong brown clays with few sands	Clay	High plasticity
BH9	38	CH	A-7-6	Dark brown clays with few sands and traces of gravels	Clay	Very high plasticity
BH10	41	CH	A-7-6	Dark yellowish brown clays with traces of sands and gravels	Clay	Very high plasticity
BH11	48	ML	A-7-5	Dark brown sandy silts with traces of gravels	Clay	Medium plasticity
BH12	51	ML	A-7-5	Very dark brown sandy silts with few gravels	Clay	Medium plasticity
BH13	53	CH	A-7-6	Very dark clays with little sands	Clay	High plasticity

Table 8. Cohesion and Friction Angle.

Sampling Code	Actual Slope (°)	Soil Classification (USCS)	Cohesion (kN/m <sup>2</sup> )	Friction Angle (°)
BH1	6	MH	11.4	16.9
BH3	13	CH	19.8	10.8
BH7	27	ML	16.1	15.7
BH12	51	ML	23.1	8.0

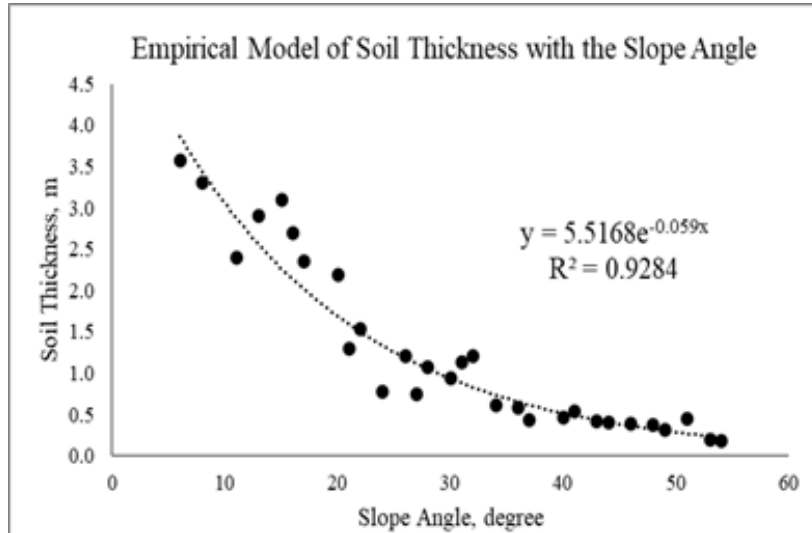


Figure 4. Correlation of Soil Thickness with the Slope Angle (Daleon & Lorenzo, 2018).

Table 9. Predicted Soil Thickness

SLOPE	ACTUAL SOIL THICKNESS	PREDICTED SOIL THICKNESS
6	2.93	3.85
11	1.77	2.83
13	2.27	2.50
20	1.02	1.59
21	0.68	1.49
26	0.44	1.07
27	0.54	1.00
31	0.82	0.76
38	0.37	0.46
41	0.41	0.37
48	0.70	0.22
51	0.46	0.17
53	0.40	0.15

Figure 4 illustrates the relationship between soil thickness and slope angle within the study area. This relationship is described by an exponential correlation, suggesting that soil thickness decreases exponentially with increasing slope angle. This trend is consistent with geomorphological principles, as steeper slopes often have thinner soil layers due to increased erosion and less accumulation of soil particles. The exponential correlation yielded a high coefficient of determination,  $R^2 = 0.9284$ . A high R-squared value, close to 1, suggests that the

regression line closely fits the data. The high R-squared value indicates that the exponential correlation is a good model for predicting values of the soil thickness needed in slope stability analysis. Soil thickness is a critical parameter in slope stability, influencing the weight of the soil and the potential driving forces for slope failure.

Table 9 presents the predicted soil thickness values for the study area. These values were calculated using the equation derived from the correlations established

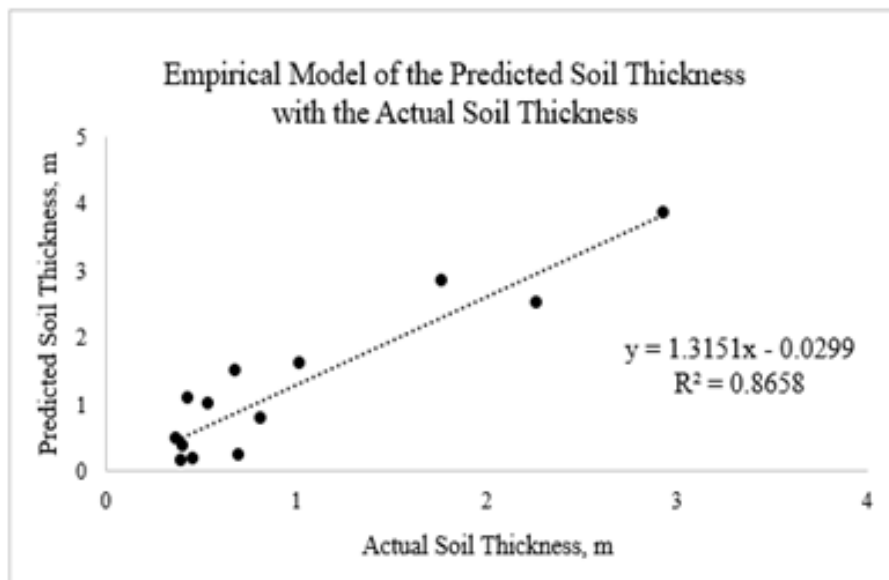


Figure 5. Correlation of Predicted Soil Thickness with the Actual Soil Thickness.

by Daleon & Lorenzo (2018). This equation allowed for a systematic and consistent estimation of soil thickness across the study area.

The validity of the predicted soil thickness was confirmed through exponential correlation, as illustrated in Figure 5. This method was chosen due to its ability to model the relationship between the predicted soil and the actual soil thickness. The exponential correlation yielded a high coefficient of determination with a value of  $R^2 = 0.8658$ , thereby affirming the accuracy of the soil thickness predictions.

#### *Slope Stability Assessment*

The result of the slope stability assessment is presented in two sections. These two conditions represent a spectrum of possible scenarios, from less severe to a worst-case scenario, and provide a comprehensive understanding of the slope's response under various circumstances. This assessment uses specific parameters, which include the friction angles ( $\Phi$ ) and the factor of safety (FS), to understand the degree of slope stability in different circumstances. The first section discusses the FS distribution under semi-saturated conditions, where  $m_1 = 0.25$  and  $m_2 = 0.5$ . The second section focuses on the fully saturated condition, with  $\Phi$  of 2.6, 4.4, 6.4, 8.7, and 0.

In the semi-saturated condition, the computed FS values for  $m_1 = 0.25$  and  $m_2 = 0.50$  are all greater than two, indicating a very high level of slope stability. Figures 6 and 7 show the robustness of the slope under these conditions. Under fully saturated conditions, the FS values vary depending on the friction angle. For friction angles of 2.60, 4.40, and 6.40, the FS values range from 1.5-2 to greater than 2, indicating a high to very high slope stability, as shown in Figures 8, 9, and 10. A friction angle of 8.70 yields very high slope stability, with FS values exceeding 2, as depicted in Figure 11. Even in a potentially catastrophic scenario where the  $\Phi$  is equal to zero, the FS values range from 1.5-2 to greater than 2, suggesting a high to very

high slope stability, as shown in Figure 12.

Despite the generally favorable results, it is essential to remember that slope stability is not guaranteed under all circumstances. For instance, in 2014, continuous rainfall from June 1 to 10 led to numerous landslide incidents in the Municipality of Kibawe, Bukidnon. Although no casualties were reported in Barangay Kiorao, the incidents are a stark reminder of the potential dangers of unstable slopes. Several research studies emphasize the conditional stability of slopes, even those with FS greater than 1 (Mugagga et al., 2012). Both internal and external factors can influence the stability of the soil. In particular, highly plastic inorganic soils can become prone to sliding during rainfall due to reduced shear resistance (Dai et al., 2002). External variables such as high rainfall, deforestation, farming, and excavation can lead to slope instability even in previously considered stable areas (Mugagga et al., 2012).

Thus, while the current assessment provides strong indicators of slope stability, it is crucial to remember that this is not a guarantee. Given the many factors influencing slope stability, it remains a complex and nuanced issue requiring continual monitoring and assessment.

#### *Geohazard Mapping*

HazardHunterPH, a leading authority in seismic hazard assessment, has thoroughly investigated and pinpointed Kiorao Elementary School as a critical facility in Kibawe, Bukidnon. The school's location, approximately 18.4km from the South Bukidnon Fault, ensures its safety from the threat of ground rupture, a common occurrence during seismic activities along fault lines. In addition to its safety from ground ruptures, the school's geographical position also safeguards it from the risks of liquefaction and tsunamis. Liquefaction, a process where saturated soil temporarily loses strength and behaves as a fluid during intense ground shaking, is not a concern for the school due to its geographical position. Similarly,

the threat of tsunamis, often triggered by undersea earthquakes, is also negligible. However, despite these safety assurances, the school is only partially immune to the effects of seismic activity. It remains vulnerable to ground shaking, a common earthquake phenomenon that can cause significant structural damage. Updates on the vulnerability to earthquake-induced landslides are still unavailable. However, it is known to be highly susceptible to rain-induced landslides. This susceptibility is apparent by numerous old or inactive landslides in the vicinity, indicating the area's instability during periods of heavy rainfall.

Geohazards, such as those mentioned above, play a pivotal role in land development. Ignoring these hazards during the early planning stages can result in severe consequences, including structural damage, financial losses, and even loss of life. Therefore, it is crucial to incorporate geohazard considerations into the planning process from the outset. The geohazard map is a valuable tool in this regard. It provides detailed information about slope

gradients vulnerable to instability based on their safety factor. This data allows planners to avoid constructing on slopes likely to fail under certain conditions. The map also indicates the potential for soil collapse, another critical consideration in land development.

Furthermore, the geohazard map pinpoints the locations of active and potentially active faults. This information is crucial for avoiding construction near these hazardous areas. Figure 13 visually represents these geohazards, making it easier for planners and developers to understand the risks involved.

A geohazard map is an indispensable tool for evaluating potential risks and creating a comprehensive picture of a community's vulnerability to geological hazards. It can be utilized for preliminary assessments and reviews of land development projects during the early planning stages. Using this tool effectively, planners and developers can mitigate risks, ensure safety, and promote sustainable development.

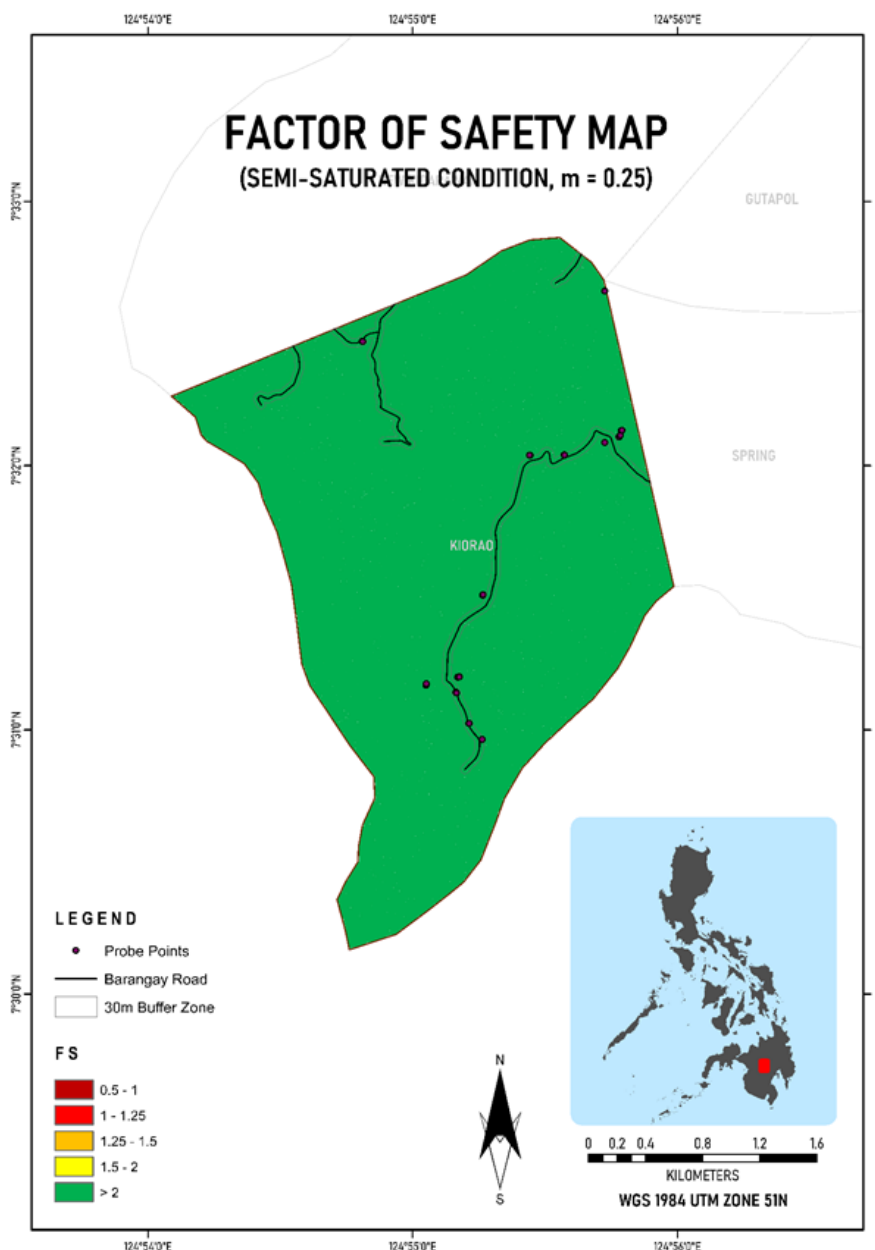


Figure 6. The Factor of Safety Map (Semi-saturated Condition,  $m = 0.25$ ).

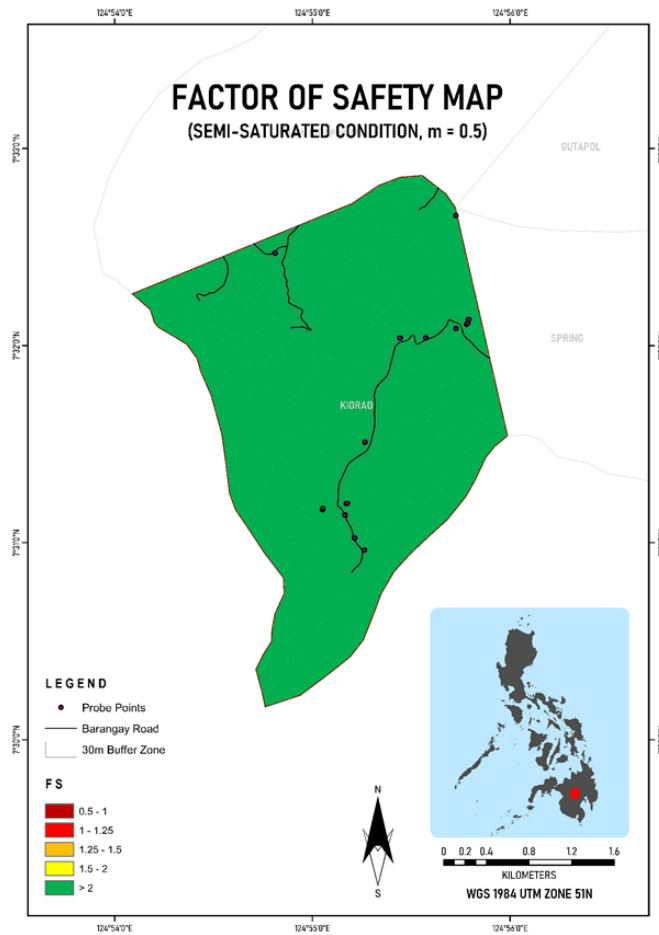


Figure 7. The Factor of Safety Map (Semi-saturated Condition,  $m = 0.50$ ).

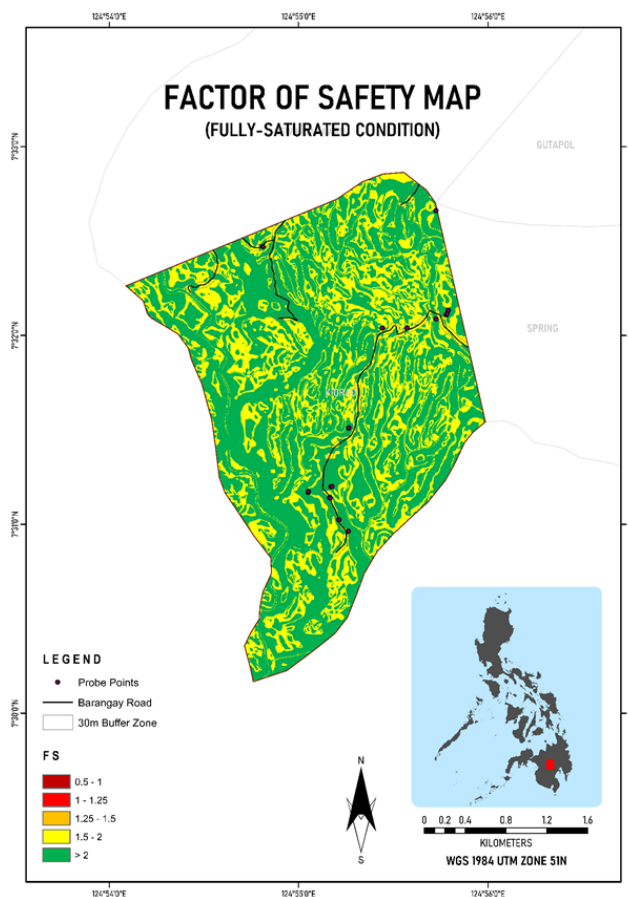


Figure 8. The Factor of Safety Map (Fully-saturated Condition, friction angle = 2.60).

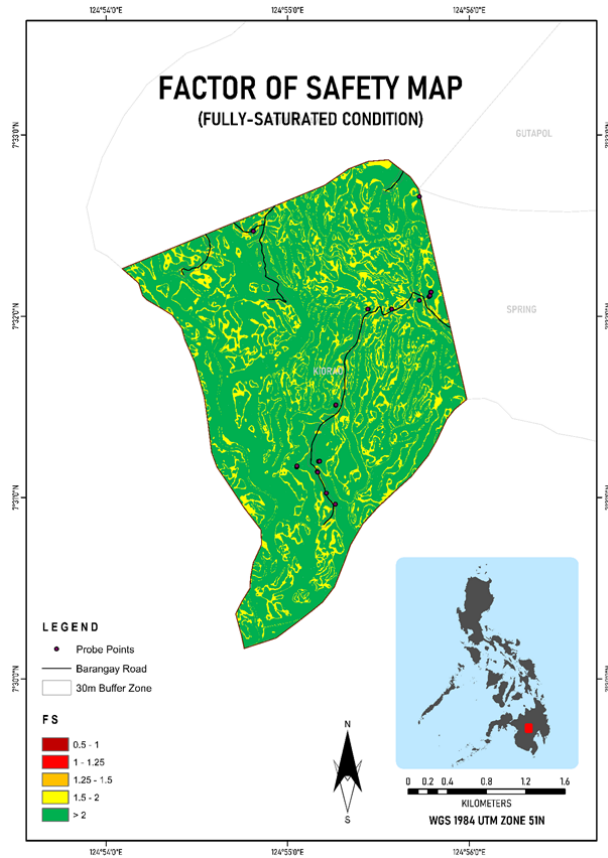


Figure 9. The Factor of Safety Map (Fully-saturated Condition, friction angle = 4.40).

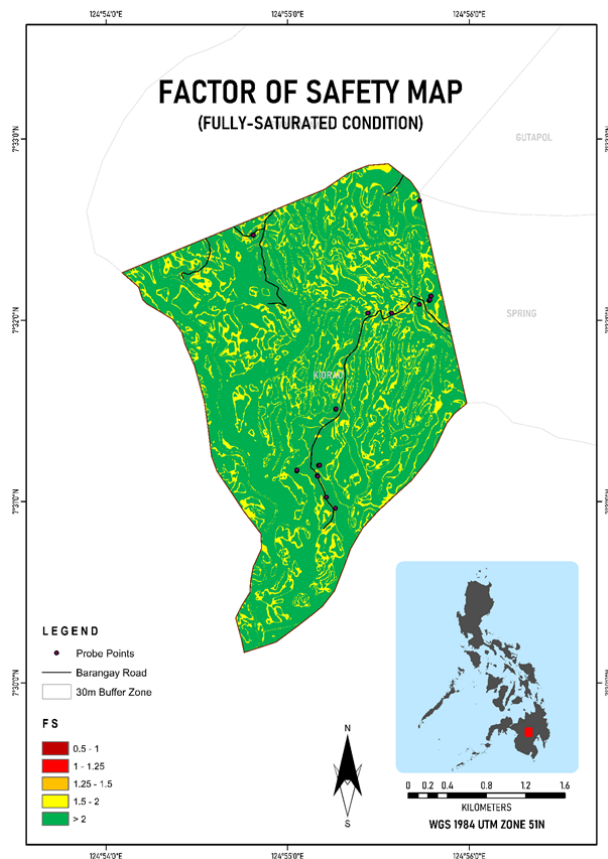


Figure 10. The Factor of Safety Map (Fully-saturated Condition, friction angle = 6.40).

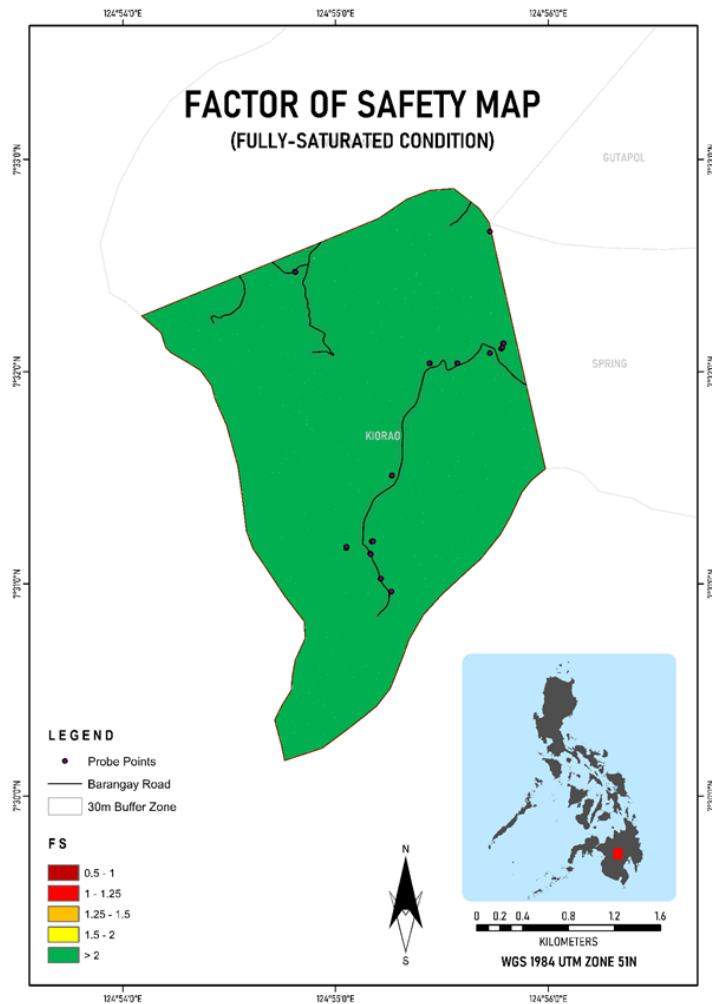


Figure 11. The Factor of Safety Map (Fully-saturated Condition, friction angle = 8.70).

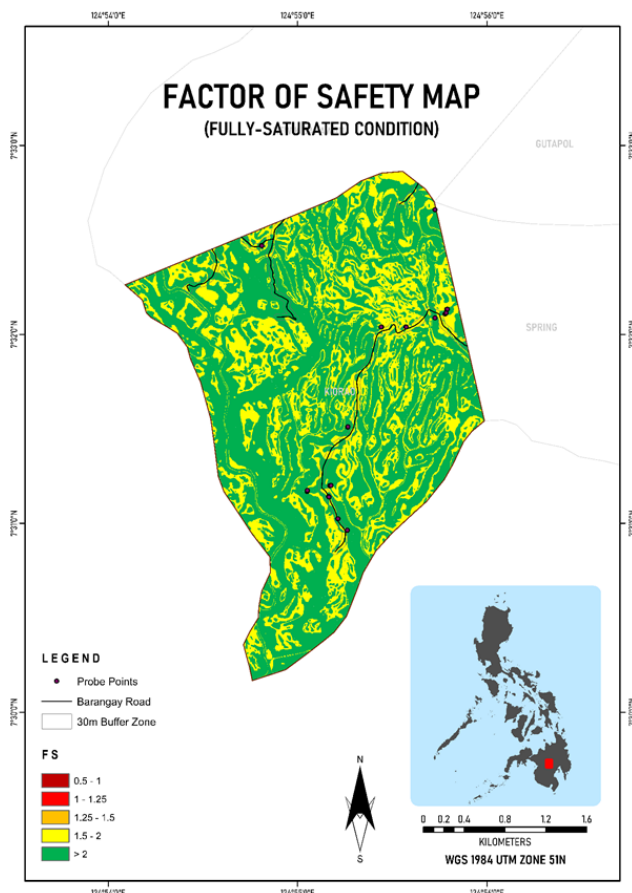


Figure 12. The Factor of Safety Map (Fully-saturated Condition, friction angle = 0).

# GEOHAZARD MAP

KIORAO, KIBAWE, BUKIDNON

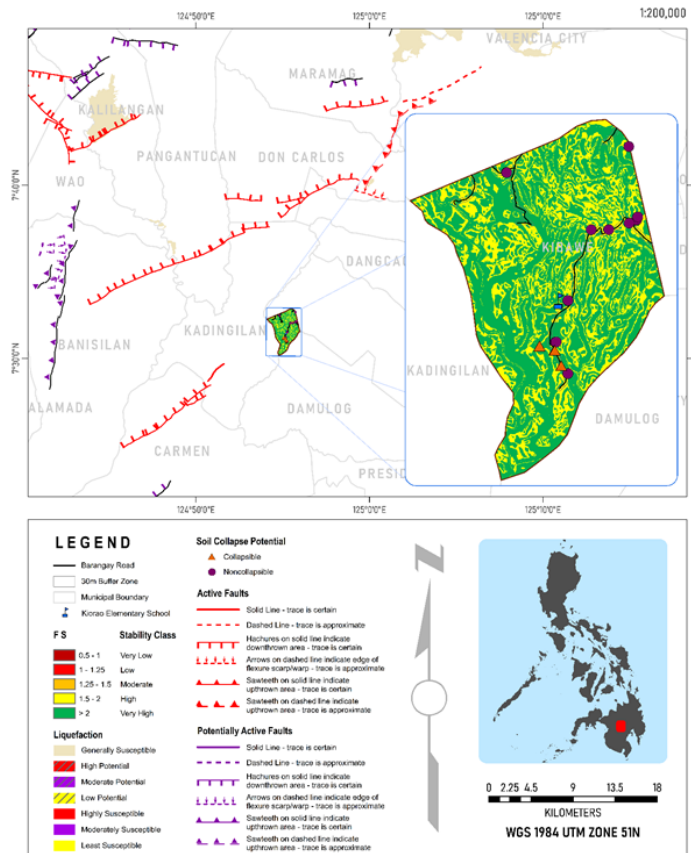


Figure 13. Geohazard Map of Barangay Kiorao, Kibawe, Bukidnon.

## CONCLUSION

The study successfully assessed the geohazards of Barangay Kiorao, Kibawe, Bukidnon, providing valuable insights for land development planning and risk management. The study revealed that the FS values for the semi-saturated conditions with  $m_1 = 0.25$  and  $m_2 = 0.50$  are all greater than two, indicating very high slope stability. For the fully saturated conditions, the FS values with friction angles equal to 0, 2.60, 4.40, and 6.40 range from 1.5-2 to greater than 2, suggesting high slope stability. The FS values for the fully saturated condition with a friction angle equal to 8.70 are greater than 2.0, indicating very high slope stability.

The soil in the study area is identified as soft clay, which is highly expansive and has the propensity to swell. This could have significant implications for land development in the area. Furthermore, three locations in the study area are classified as collapsible. These areas could be at risk of sudden and dramatic settlement, which could pose a risk to any structures built on them. Land development in the area should consider the expansive and collapsible nature of the soil.

The seismic hazard assessment identified Kiorao Elementary School as one of the nearest critical facilities in Kibawe, Bukidnon. The school is safe from ground rupture, but it

could still be vulnerable to ground shaking. The school should be equipped with earthquake-resistant features and earthquake drills should be conducted regularly.

Finally, the study generated a geohazard map showing information regarding the slope gradients vulnerable to instability based on their FS and the location of active and potentially active faults. This map is a valuable tool for land development planning and risk management. It identified areas at high risk of geohazards and guided decisions about where to build and avoid.

## ACKNOWLEDGMENT

The author would like to acknowledge Central Mindanao University for funding this research and the local government unit of the Municipality of Kibawe, Bukidnon, headed by Hon. Reynaldo S. Ang Rabanes; the mayor, and to and to Hon. Raymundo A. Batao Jr., the vice mayor of Kibawe, Bukidnon, for their commitment and confidence in the researchers.

## REFERENCES

Arca, M. C. Q., & Lorenzo, G. A. (2018). Landslide hazard mapping using limit equilibrium method with GIS application of roadway traversing mountain slopes: The case of Kitaotao Bukidnon, Philippines. *Journal of*

- Nepal Geological Society, 55(1), 93-101.
- Aurelio, M.A. (2004). Engineering Geological and Geohazard Assessment (EGGA) System for Sustainable Infrastructure Development: The Philippine Experience. *Bulletin-Geological Society of Hong Kong*, 7, 33-39.
- Baynes, F. J. (2008). Anticipating problem soils on linear projects. In *Conference proceedings on problem soils in South Africa* (Vol. 34, pp. 9-21).
- Bidyashwari, H., Kushwaha, R. S., Chandra, M., & Okendro, M. (2017). Physical properties of soil and its implication to slope stability of Nungbi Khunou, NH-150, Manipur. *International Journal of Geosciences*, 8(11), 1332.
- Bláhová, K., Ševelová, L., & Pilařová, P. (2013). Influence of water content on the shear strength parameters of clayey soil in relation to stability analysis of a hillside in Brno region. *Acta Universitatis Agriculturae et Silviculturae Mendelianae Brunensis*, 61(6), 1583-1588.
- Chae, B. G., Lee, J. H., Park, H. J., & Choi, J. (2015). A method for predicting the factor of safety of an infinite slope based on the depth ratio of the wetting front induced by rainfall infiltration. *Natural Hazards and Earth System Sciences*, 15(8), 1835-1849.
- Craig, R. F. (1997). *Soil Mechanics*. E & FN Spon. London, UK.
- Dai, F. C., Lee, C. F., & Ngai, Y. Y. (2002). Landslide risk assessment and management: an overview. *Engineering geology*, 64(1), 65-87.
- Daleon, C. F. (2022). Soil Characterization Based on Physical and Mechanical Properties of Pliocene-Pleistocene Geology in Bukidnon Philippines. *European Journal of Environment and Earth Sciences*, 3(2), 61-67.
- Daleon, C. F., & Lorenzo, G. A. (2018). Empirical models for predicting the spatial variation of soil thickness and shear strength for landslide susceptibility assessment. *Journal of Nepal Geological Society*, 55(1), 85-91.
- Department of Environmental and Natural Sciences, Mines and Geosciences Bureau, Region 10. (2013). 1:10,000 Scale Geohazard Maps of Bukidnon. Retrieved from <http://www.mgb10.com/mgb10/2013/05/29/110000-scale-geohazard-maps-of-bukidnon/>.
- Der Merwe, V. (1964). The prediction of heave from the plasticity index and the percentage clay fraction. *The Civil Engineer in South Africa*, 6(6), 103.
- Griffiths, D. V., Huang, J., & Fenton, G. A. (2011). Probabilistic infinite slope analysis. *Computers and Geotechnics*, 38(4), 577-584.
- Holtz, W. G., & Gibbs, H. J. (1967). Research related to soil problems of the arid western United States. *Proceedings of the Third Pan-American Conference on Soil Mechanics and Foundation Engineering*, Caracas.
- Ian, J., & Chris DF, R. (2012). Chapter 32 Collapsible soils. In *ICE manual of geotechnical engineering* (pp. 391-411). Thomas Telford Ltd.
- Kabeta, W. F., & Lemma, H. (2023). Modeling the application of steel slag in stabilizing expansive soil. *Modeling Earth Systems and Environment*, 1-8.
- Mason, P. J., & Rosenbaum, M. S. (2002). Geohazard mapping for predicting landslides: an example from the Langhe Hills in Piemonte, NW Italy. *Quarterly Journal of Engineering Geology and Hydrogeology*, 35(4), 317-326.
- Muço, B., Alexiev, G., Aliaj, S., Elezi, Z., Grecu, B., Mandrescu, N., ... & Shkupi, D. (2012). Geohazards assessment and mapping of some Balkan countries. *Natural hazards*, 64, 943-981.
- Mugagga, F., Kakembo, V., & Buyinza, M. (2012). A characterization of the physical properties of soil and the implications for landslide occurrence on the slopes of Mount Elgon, Eastern Uganda. *Natural hazards*, 60(3), 1113-1131.
- O'Kelly, B. C. (2021). Review of recent developments and understanding of Atterberg limits determinations. *Geotechnics*, 1(1), 59-75.
- Opiso, E. M., Puno, G. R., Alburo, J. L. P., & Detalla, A. L. (2016). Landslide susceptibility mapping using GIS and FR method along the Cagayan de Oro-Bukidnon-Davao City route corridor, Philippines. *KSCE Journal of Civil Engineering*, 20, 2506-2512.
- Padrones, J. T., Ramos, N. T., Dimalanta, C. B., Queaño, K. L., Faustino-Eslava, D. V., Yumul, G. P., & Watanabe, K. (2017). Landslide susceptibility mapping in a geologically complex terrane: a case study from northwest Mindoro, Philippines. *Manila J Sci*, 10, 25-44.
- Philippine Statistics Authority, 2015 Census of Population, Report No. 3 – Population, Land Area, and Population Density. Retrieved from [https://www.psa.gov.ph/sites/default/files/\\_POPCEN%20Report%20No.%203.pdf](https://www.psa.gov.ph/sites/default/files/_POPCEN%20Report%20No.%203.pdf).
- Selby, M. J. (1993). *Hillslope Materials*. Oxford University Press, 451p.
- Wang, Z. (2011). Seismic hazard assessment: issues and alternatives. *Pure and Applied Geophysics*, 168, 11-25.